Atmos. Chem. Phys., 4, 511–521, 2004
www.atmos-chem-phys.org/acp/4/511/
SRef-ID: 1680-7324/acp/2004-4-511

Atmospheric Chemistry and Physics

Observations of meteor-head echoes using the Jicamarca 50 MHz radar in interferometer mode

J. L. Chau and R. F. Woodman

Radio Observatorio de Jicamarca, Instituto Geofísico del Perú, Lima

Received: 1 October 2003 – Published in Atmos. Chem. Phys. Discuss.: 28 November 2003
Revised: 4 March 2004 – Accepted: 11 March 2004 – Published: 24 March 2004

Abstract. We present results of recent observations of meteor-head echoes obtained with the high-power large-aperture Jicamarca 50 MHz radar (11.95° S, 76.87° W) in an interferometric mode. The large power-aperture of the system allows us to record more than 3000 meteors per hour in the small volume subtended by the 1° antenna beam, albeit when the cluttering equatorial electrojet (EEJ) echoes are not present or are very weak. The interferometry arrangement allows the determination of the radiant (trajectory) and speed of each meteor. It is found that the radiant distribution of all detected meteors is concentrated in relative small angles centered around the Earth's Apex as it transits over the Jicamarca sky, i.e. around the corresponding Earth heading for the particular observational day and time, for all seasons observed so far. The dispersion around the Apex is ∼18° in a direction transverse to the Ecliptic plane and only 8.5° in heliocentric longitude in the Ecliptic plane both in the Earth inertial frame of reference. No appreciable interannual variability has been observed. Moreover, no population related to the optical (larger meteors) Leonid showers of 1998–2002 is found, in agreement with other large power-aperture radar observations.

A novel cross-correlation detection technique (adaptive match-filtering) is used in combination with a 13 baud Barker phase-code. The technique allows us to get good range resolution (0.75 km) without any sensitivity deterioration for the same average power, compared to the non-coded long pulse scheme used at other radars. The matching Doppler shift provides an estimation of the velocity within a pulse with the same accuracy as if a non-coded pulse of the same length had been used. The velocity distribution of the meteors is relatively narrow and centered around 60 km s^{-1}. Therefore most of the meteors have an almost circular retrograde orbit around the Sun. Less than 8% of the velocities correspond to interstellar orbits, i.e. with velocities larger than the solar escape velocity (72 km s^{-1}). Other statistical distributions of interest are also presented.

Correspondence to: J. L. Chau
(jchau@jro.igp.gob.pe)

1 Introduction

High-power large-aperture (HPLA) radars frequently detect very fast meteor head echoes with a range-rate velocity which follows the meteoroid as it travels through the upper atmosphere. Although meteor "head echoes" were first observed in the late 1940s, this topic has become an area of interest only recently as scientists have focused more intensely on the importance and usefulness of meteors (e.g. Chapin and Kudeki, 1994; Mathews et al., 1997; Zhou et al., 1998; Wannberg et al., 1996; Close et al., 2002a,b; Janches et al., 2003). Head echo measurements give accurate radial velocities (along the radar line of sight) and altitude ranges of deposition. Measurements are also provided – with varying degrees of accuracy – for transverse velocities, deceleration rates, and signal strengths as a function of altitude. The powerful narrow-beam radars which measure head echoes detect far more and smaller meteors than do classical meteor radars (e.g. Hocking et al., 2001). The use of these radars allows us to study the population of meteors which probably contributes the most extraterrestrial material to the Earth's upper atmosphere.

One of the main drivers for the increasing interest on meteor studies has been the presence in recent years of spectacular optical Leonid meteor showers. At Jicamarca that was not an exception and meteor observations, particularly of head echoes, have been carried out since November 1998.

Meteor studies have been particularly difficult over Jicamarca due to the presence of very strong equatorial electrojet (EEJ) echoes (e.g. Farley, 1985b) and non-specular trail echoes (e.g. Chapin and Kudeki, 1994). This geophysical "clutter" (for meteor head echo studies) occur at similar

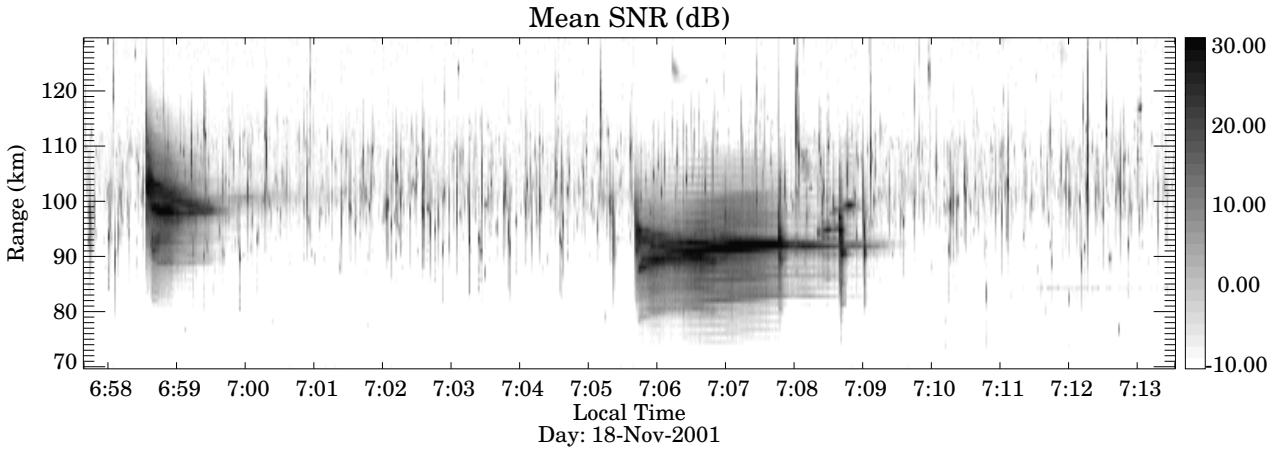

Fig. 1. Range-time intensity plot of meteor echoes. Head echoes are represented by the vertical gray striations (∼1 per second). Examples of long-lived meteor trails occur around 06:59 and 07:06 LT.

Table 1. Radar parameters for observing meteor-head echoes at Jicamarca.

Parameter	Value	Units
Inter pulse period (IPP)	200	km
Pulse width	9.75	km
Barker code	13	
Sampling rate	0.75	km
Initial range	70	km
Number of samples	92	
Number of complex channels	4	
Transmitter peak power	2	MW

altitudes where most head echoes are expected (between 90 and 120 km). Nonetheless, with the recent improvements of our acquisition systems, we have started the head echo observations around sunrise times when there is not only an increase in the rate of meteor observations but also when EEJ echoes are expected to be weaker or sporadic.

In Fig. 1 we show an example where meteor head echoes are observed at the same time when long-lived non-specular meteor trail echoes are present (around 06:59 and 07:06). All the striations in light gray represent head echoes (∼1 head-echo per second). Although in this work we discuss the head echo results, the long-lived (Chapin and Kudeki, 1994) and the non-specular (Dyrud et al., 2002) meteor trails are being studied independently (M. Oppenheim, personal communication).

As we show below, Jicamarca offers unique observations to the world-wide effort of improving the understanding of the physical origin and orbits of the meteors. It has the lowest frequency of all the high-power large-aperture radars (50 Mhz), it is located under the magnetic equator (11.95° S, 76.87° W) and it is able to measure the three dimensional vector of head echoes by operating in the interferometer mode (e.g. Woodman, 1971). The MU radar (34.85° N, 136.11° E) (Sato et al., 2000) and the ALTAIR radar (9° N, 167° E) (Close et al., 2002a) are also able to determine the three dimensional vector velocity but both of them with smaller transmitting antennas.

Our paper is organized as follows. First we present a description of the experimental setup. Then we describe our technique, including the decoding process that allows us not only to improve the range resolution but also the meteor detection. In addition we present the meteor characterization process. Results from Leonid and non-Leonid observations are presented and discussed, particularly related to their impact trajectory statistics. Finally we summarize our results and conclusions.

2 Experimental setup

Meteor-head observations have been made using the large Jicamarca array (∼300 m×∼300 m) for transmission and all four quarter sections for reception (∼75 m×∼75 m). The same linear polarization (NE) has been used in both modes. The antennas were phased to point on-axis, i.e. ∼−1.46° off-vertical in the y-direction (see Fig. 2).

Although complex voltages (raw data) from four quarters were recorded, we only need the information of three non-collinear antennas in order to locate the meteors inside the transmitting beam. For the results we present in this paper, we have used quarters A, C, and D to get the direction cosines of meteors with respect to the x- and y-axis. Note that the x-axis is rotated with respect to the East-West baseline ∼51.06°.

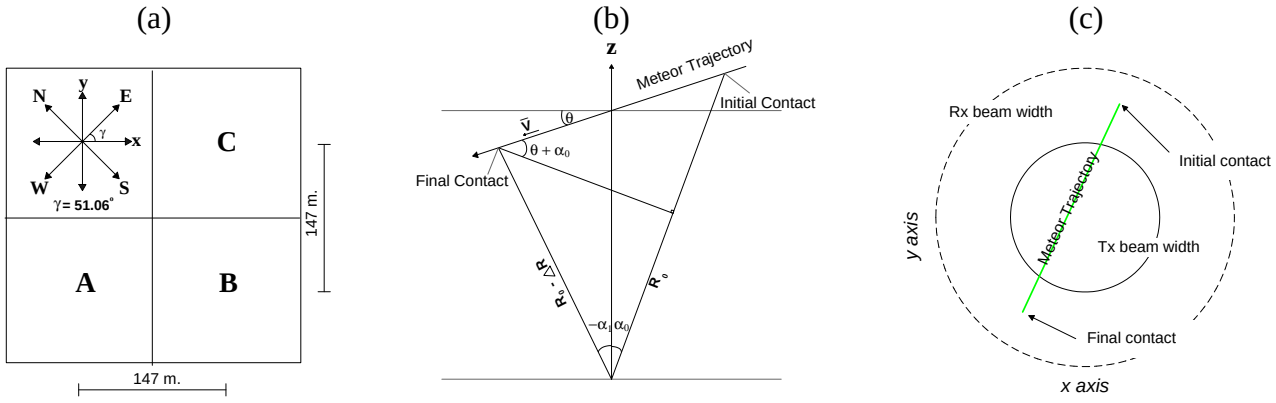

Fig. 2. (a) Antenna configuration for interferometric observations of meteors, note that the x-axis is rotated with respect to the East-West baseline ∼51.06°. Simplified geometry of a meteor trajectory with respect to the illuminated beam: **(b)** altitudinal and **(c)** horizontal views.

Figures 2b and c show a simplified diagram of a meteor trajectory inside the illuminated beam as a vertical cut in the plane of the meteor trajectory and a plan view, respectively. The actual transmitting half-power beam width is ∼1°.

The main radar parameters for the meteor mode are summarized in Table 1. We have used the full duty cycle available (5%) and a reasonable high range resolution by using a 13-bit Barker code (0.75 km baud).

3 Technique description

As it was mentioned in the introduction meteor-head echoes come from altitudes where strong geophysical "clutter" due to EEJ and non-specular meteor trail echoes occur. Therefore, special observing and processing modes are needed to try to overcome this clutter. Our observing mode consists on (1) trying to operate when the EEJ echoes are absent or weak (e.g. around sunrise or during counter EEJ conditions), (2) using interferometry, (3) using pulse coding, and (4) recording raw data. The processing mode is described below.

Once the raw data has been recorded, we proceed off-line to obtain the parameters of meteor-head echoes. We have divided our processing technique in three different stages: (a) decoding, (b) signal statistics and meteor detection, and (c) meteor characterization.

3.1 Decoding

Usually coded pulses are used in order to improve the range resolution without sacrificing the maximum average power of the transmitter. In most applications, where the targets are quasi-stationary the decoding procedure is performed by correlating with the same code use for transmission (e.g. Farley, 1985a). In the case of meteor-head echo observations, the large Doppler shift does not allow the use of a simple correlation with the transmitter pulse shape (e.g. Wannberg et al., 1996). Proper decoding requires cross-correlating with the transmitter phase coded pulse but Doppler shifted by the radial velocity of the meteor. Since we are cross-correlating with the expected shape of the echo, we have actually an optimum cross-correlation detection scheme. Nonetheless, the actual radial velocity of the meteor is not known, therefore one needs to perform a search. The search is performed by cross-correlating with different Doppler shifts. The velocity that produces the optimum decoding is an estimate of the radial velocity of the meteor. Thus, the decoding is not only used for improving the range resolution but also for estimating the meteor radial velocities.

The expected range of radial velocities of meteor head echoes is very large, between 10 and 80 km/s. Normally a search within this range would be a lengthy procedure. A way around this is to use a traditional pulse-to-pulse method, as used in most coherent scatter applications. This technique would normally produce a more accurate velocity estimate because of the larger time span involved. Indeed it does, but for several discrete ambiguous values, but not as many as the complete range of continuous possible velocities mentioned above.

The approach we have used is a combination of both. A search is made with the few discrete velocities obtained from the pulse-to-pulse technique and the one that produces maximum correlation is selected for each raw data profile. If the uncertainty in defining the maximum correlation is small enough to discriminate between adjacent ambiguous velocities, the technique would produce velocities as accurate as those obtained with the pulse-to-pulse technique, and at the same time a proper velocity for optimum decoding. Unfortunately, for the IPP we have used, i.e. a Nyquist limit of $\pm 1.5\,\mathrm{km\,s^{-1}}$, the uncertainty in the maximum correlation does not allow us to discriminate between the two unambiguous possible values which produce the two maximum values. As a consequence, the accuracy achieved is that of the maximum cross-correlation technique. We plan to use in the future much shorter and aperiodic IPPs to better exploit the

more accurate velocities obtained with multiple-pulse techniques.

Another way to determine the velocity is by using a long pulse (e.g. Sato et al., 2000; Janches et al., 2003). However, this approach is not suitable at Jicamarca due to the presence of geophysical clutter at similar altitudes. Our approach, i.e. coded long pulse, has comparable sensitivity and Doppler velocity accuracy as the non-coded long-pulse. As we mentioned above, much better velocity accuracy is obtained from the pulse-to-pulse measurements which we have used to get the decelerations.

Barker decoding, including the proper Doppler correction mentioned above, produces range sidelobes of -22 dB with respect to the mainlobe. It is possible to reduce the magnitude of the sidelobes by additional filtering at the expense of spreading the sidelobe contamination into more ranges. We have used a second filter on the decoded raw data profiles to decrease further the peak to sidelobe levels (from -22 dB to less than -32 dB) (e.g. Rihaczek and Golden, 1971). This second filter is needed in order improve the discrimination between head and the geophysical clutter, i.e. meteor trail and EEJ echoes.

3.2 Signal statistics and meteor detection

Once the Doppler velocity for optimum decoding ($v_{\rm opt}(t)$) is found, the raw voltages (V_i) for each of the channels i is decoded. Then, the following signal statistics are recorded along with $v_{\rm opt}(t)$ for later processing,

$$\rho_{i,j}(r, t:0) \text{ for } i,\ j = 0, 1, 2, 3 \quad (1)$$

$$\rho_{i,i}(r, t:\tau) \text{ for } i = 0, 1, 2, 3, \quad (2)$$

where $\rho_{i,j}(r, t{:}\tau) = <V_i(r, t) V_j^*(r, t+\tau)>$ is the cross-correlation between complex channels corresponding to antennas i and j at range r and delay τ, $<>$ represents emsemble averages of 4 (3) IPPs for τ=0 (τ=1 IPP) in this work. As we show later, the statistics at $\tau \neq 0$ (equal to one IPP) are used to calculate a pulse-to-pulse Doppler velocity with good accuracy, but ambiguous.

Once all the signal statistics are recorded (needed for careful processing of meteor trail echoes), we proceed by finding the range (r_p) where the power is maximum for each profile ("peak"). Then, the peak signal statistics of probable head echoes are recorded, i.e. $\rho_{i,j}(r_p, t{:}0)$, $\rho_{i,i}(r_p, t{:}\tau)$, $v_{\rm opt}(t)$, in addition to $r_p(t)$.

3.3 Meteor characterization

Working with the peak signal statistics is much faster than working with the raw data, allowing us to test and implement robust algorithms for meteor characterization. Given the large number of head echoes, we have implemented an algorithm that is based on our experience after observing many of them very carefully. For example, among other criteria, we do not consider meteors moving away from the radar, or with positive radial accelerations. A probable meteor-head echo has to be present for a minimum time interval in order to be considered. At this point, our approach has been very conservative in the sense that if a head echo is not well defined, then it is rejected. For example, we have observed cases where two or more head echoes are present at the same time but at different ranges, in such cases, we reject all of them since a more intelligent algorithm is needed to characterize them. After this rejection process, we are observing $\sim$3000 meteor heads per hour.

From the peak signal statistic recorded we obtained directly the following meteor parameters:

1. Initial range (R_0)
2. Range coverage (ΔR)
3. Duration of meteor event (Δt)
4. Mean signal-to-noise ratio (SNR)
5. Radial velocity (v_r). This parameter is measured using three independent methods: (a) from the first moment of the pulse-to-pulse statistics (v_{ra}), (b) from fitting a straight line (range versus time) of the meteor trajectory (v_{rb}), (b) from the average $v_{\rm opt}$ along the observable meteor trajectory (v_{rc}).

   As we mentioned above, the radial velocity from pulse-to-pulse is ambiguous because of the relatively long sampling period used (Nyquist theorem), however, it has very small uncertainties (e.g. Woodman, 1985).

   The correlation between the last two methods (v_{rb} vs. v_{rc}) is very high ($>$0.92) but there is a bias that varies between 2 and 6 km s^{-1} ($v_{rb} < v_{rc}$) whose origin we still do not understand. Below we will use v_{rc} for v_r, and v_{ra} to get the radial accelerations.
6. Radial deceleration (a_r). This parameter is obtained from the pulse-to-pulse radial velocity by fitting a line to v_{ra} versus time.
7. Azimuth (ϕ) and angular coverage ($\Delta\alpha$). Using interferometry on the cross-correlation statistics between antennas, we have calculated the direction cosines (θ_x, θ_y) of the meteor position at any given time with respect to the x- and y-directions. Then, the azimuth direction is obtained, again, by fitting a constant azimuth line to the set of points (θ_x, θ_y) corresponding to different times. The angular coverage ($\Delta\alpha = \alpha_0 + \alpha_1$ in Fig. 2b) is also obtained from this analysis.

In addition, we have derived the following parameters from the more direct ones enumerated above:

1. Elevation angle of meteor trajectory (θ) (not the elevation of where the meteor is observed!) is given by,

$$\theta \approx \arctan \frac{\Delta R}{R_0 \Delta\alpha}. \quad (3)$$

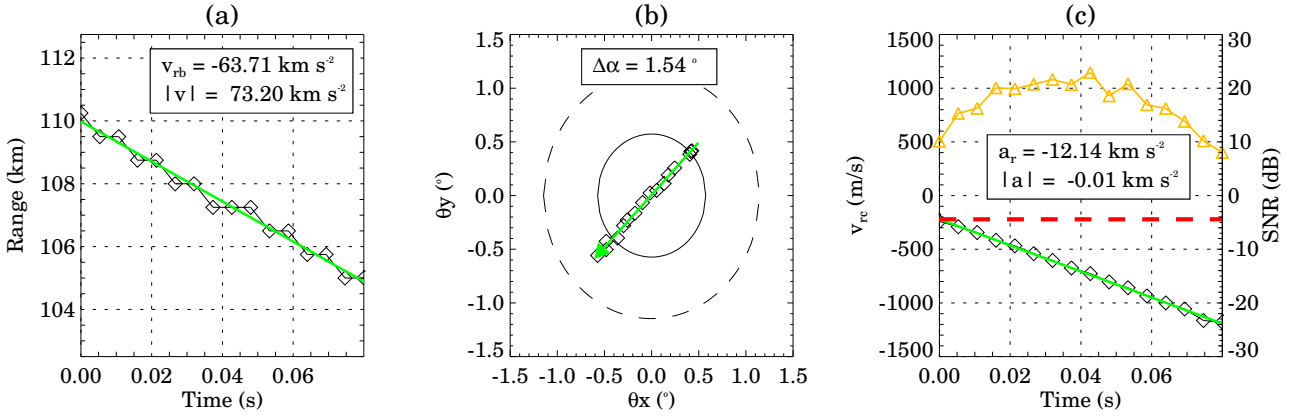

Fig. 3. Meteor characterization for most meteor events. **(a)** Range vs. time, **(b)** θ_x vs. θ_y, and **(c)** pulse-to-pulse Doppler vs. time. In all three cases the fitting lines are represented in green. In panel (c) the SNR is shown a long the meteor trajectory (scale on the right) in orange, while the absolute acceleration is given by the slope of the red line.

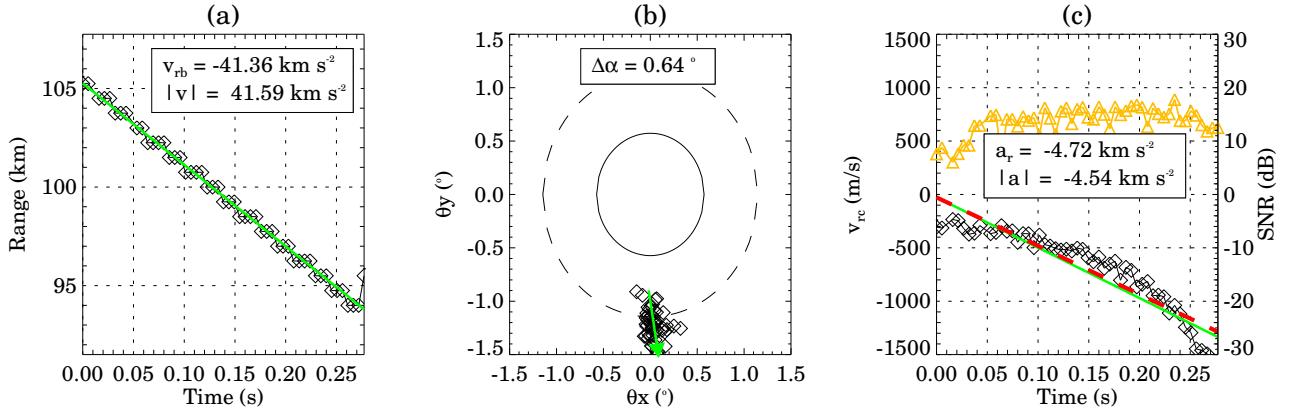

Fig. 4. Same as Fig. 3 for a meteor event with non-constant deceleration.

Here small angle approximations are used given the very narrow transmitting beam.

2. Absolute velocity ($|v|$). It is obtained from the radial velocity and the elevation angle ($|v| \sim v_r / \sin\theta$)

3. Absolute acceleration ($|a|$). As in the case of the velocity, the radar measures the radial component. Again using the small angle approximation and the geometry presented in Fig. 2b, the absolute acceleration is given by

$$|a| \approx a_r + \frac{|v|\Delta\alpha\cos\theta}{\Delta t}. \quad (4)$$

The second term comes from an apparent deceleration due to a range reduction during the meteor trajectory while it is illuminated, and which has to be corrected.

In Fig. 3 we show a typical example of how the different parameters are obtained from the (a) range vs. time diagram, (b) θ_x vs. θ_y, and (c) pulse-to-pulse radial velocity (v_{rc}) vs. time. In all three panels the fitted lines are represented in green. Figure 3c also shows the SNR along the meteor trajectory in orange (scale on the right axis) and a line with a slope equal to the absolute acceleration in red. The absolute and radial accelerations are indicated inside the box. In this particular case, we present the result of simulated meteor echo with parameters similar to most of our meteors observations (e.g. altitudinal, time, and angular coverage) and with constant velocity along its trajectory. Note that $|a|$=0 as we expected.

The great majority of our meteor observations present similar ballistic characteristics to the example shown in Fig. 3. In Fig. 4 we show a real event where the meteor lasted much longer (∼250 ms) and present a non-constant deceleration (note the exponential decay) with respect to the example

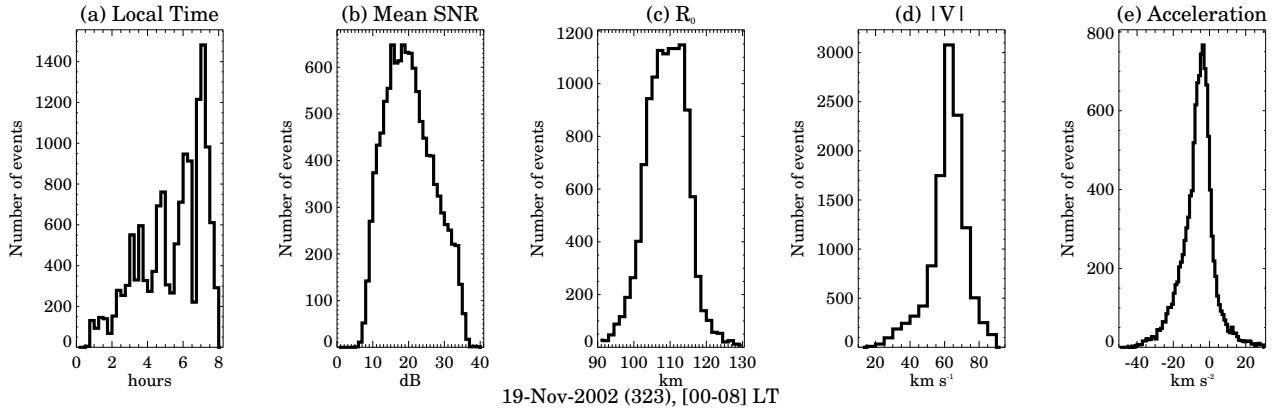

Fig. 5. Meteor statistics during 19 November 2002 when a Leonid shower occurred. **(a)** time, **(b)** mean SNR of meteor trajectory, **(c)** initial range, **(d)** absolute velocity, and **(e)** absolute acceleration.

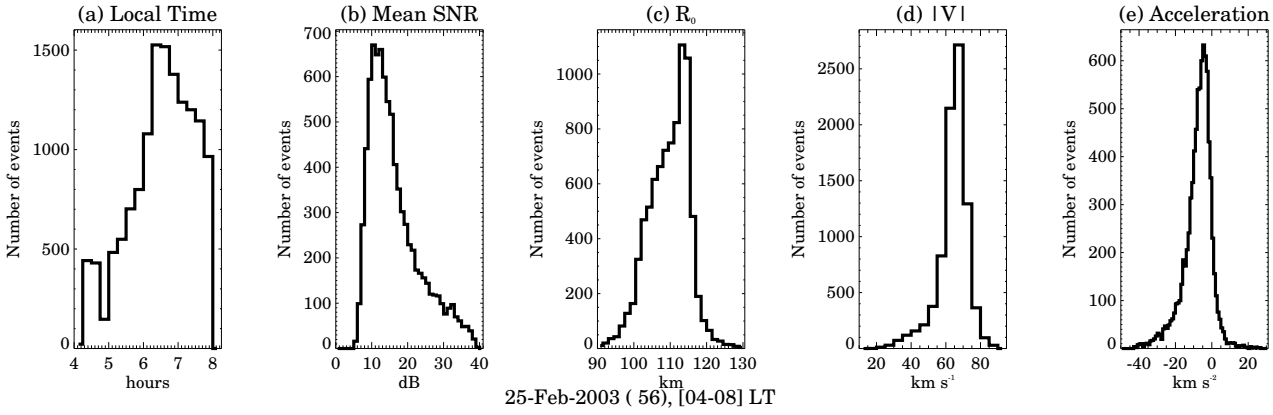

Fig. 6. Meteor statistics similar to Fig. 5 during a control night (when Leonid shower was not present) of 25 February 2003.

shown in Fig. 3. Probably the non-constant decelerations are due to the exponentially increasing atmospheric density and decreasing velocity, coupled with the shape and composition of the meteor itself. In this work we have omitted these peculiar observations by limiting the fitting errors to small numbers. However, they are interesting cases and will be treated in detail in a future work.

4 Leonid vs. non-Leonid radar observations

In this section we present the observations of 19 November 2002, when a Leonid shower occurred, and those from 25 February 2003 as a control night, sufficiently far from the shower event. Although, we have performed this type of observations around Leonid showers since 1998, the characteristics of these previous events, as far as the radar observations, are well represented by the November 2002 observations.

In Fig. 5 histograms of different parameters are shown for the Leonid night of 19 November 2002, (a) time distribution, (b) mean SNR of meteor trajectory, (c) initial range (R_0), (d) absolute velocity ($|v|$), and (f) absolute acceleration ($|a|$). In Fig. 6 similar distributions are presented for the control night of 25 February 2003.

In general, these parameters that are usually measured by other large power-aperture radars, show similar characteristics during both days: (a) occurring around 110 km, (b) mean absolute velocities are very high around 60 km s^{-1}, (c) similar SNR distributions, and (d) similar deceleration distributions. Nonetheless, these distributions are slightly different than the distributions obtained with other radars. For example, (a) our head echoes occur at higher altitudes than those observed with the Arecibo (Janches et al., 2003) and ALTAIR (Close et al., 2002a) radars; (2) we do not observe a pronounced bimodal velocity distribution (Janches et al., 2003). These differences as well as the significant number of interstellar meteors (<8%), i.e. meteors with velocities greater than 72 km s^{-1}, are currently under study.

It is important to note that most of the our meteors are moving in a retrograde direction. Moreover their orbits are around the Sun with similar parameters as the Earth (quasi

circular), since their velocities are similar to the Earth's heliocentric velocity but in opposite direction.

Our velocity distribution does not necessarily agree with the distributions obtained by classical meteor radars. As pointed out by Hunt et al. (2004) there are biases as a consequence of the lack of sensitivity to detect meteor with low mass and low velocity. But, this sensitivity is different depending on the radar technique used.

The number of events versus time distribution needs a special discussion. As we have been mentioning throughout this paper, meteor observations have been hard in the past due to the presence of strong EEJ echoes. The lack of a smooth time distribution of both days (e.g. around 05:00 LT in Fig. 6) is due to the presence of strong sporadic EEJ echoes. In any case, the maxima should be close to the actual rates, so a smooth envelope tangential to the maxima should be closer to the actual one. We plan to get a more precise time distribution in the near future, by performing similar observations over continuous days expecting that the meteor characteristics will remain almost constant during those days while the EEJ echoes will appear at different local times.

As we mentioned in the Introduction, we were motivated by the expected spectacular Leonid showers. We were hoping to contribute further knowledge on the nature of the showers with our unique observing system and geographic location. Meteors belonging to the Leonid showers are expected to have a velocity distribution around $70\,\mathrm{km\,s^{-1}}$ and a radiant clustered around a point in the Leo constellation ($\sim$10 h 8′ RA and $\sim$22° Dec) with a small angular dispersion. As can be seen from Figs. 5d and 6d, we do not observe an expected distribution enhancement with the aforementioned characteristics during the Leonid night. Moreover both days show a very similar velocity distributions.

In order to see better if the meteors were coming from the expected radiant, we have plotted the elevation and azimuth parameters in a two-dimensional graph. We have integrated this information into a conventional sky map plot commonly used by astronomers. In Fig. 7 we show a sky map distribution of meteor radiants, based on their vector velocity, around 05:00 LT on 19 November 2002. The background map shows the sky above Jicamarca ($\pm30°$ elevation) moving from left (East) to right (West) as time advances. The solid black curve represents the Ecliptic plane projected into the Celestial sphere and the thick asterisk represents the Earth's Apex. For reference, the names of the visible constellations are also indicated. The radiant, i.e. where the meteors are coming from and not where the meteors are seen in the illuminated beam, are plotted with circles. The color of the circles represents their absolute velocity (see color-coded bar in the figure) while the size is proportional to the SNR. With this type of map, we could be able to determine if a meteor shower is observed if meteors are clustered at their expected radiant and if they show their expected velocity (color).

As can be observed, the great majority of meteors are coming from the Apex at 05:00 LT. Similar result, with an increased number of meteors, is also observed around 07:00 LT in Fig. 8.

Table 2. Main parameters of angular velocity distribution around the Apex.

Parameter	Leonid night	Control night
Date	19 November 2002	25 February 2003
Period	00:00–08:00 LT	04:00–09:00 LT
Mean EW	0.08°	0.78°
Mean NS	−2.25°	1.11°
Minor axis	8.88°	8.46°
Major axis	18.05°	17.92°
Rotation with respect to EW	21.11°	−3.28°

Note that the Leo constellation is located very close to the Apex. At the beginning we thought that all the meteors were coming from Leonid. However, we observed similar results on our control nights after Leonid (not shown here). These results were puzzling until we conducted the February observations, well beyond the Leonid night.

The sky map distribution for the control night is shown in Fig. 9. Again the majority of meteors, which have very similar statistical characteristics to those observe during the Leonid night, are clustered around the Apex.

The picture that emerged from these observations is that the meteors detected by our radar are always clustered around the Apex and that the Leonid radiant happened to be within the same region during the November observations. In addition, there was no measurable increase in the total meteor population during the meteor shower, not even when a smaller region around the optical radiant and with the expected velocity was considered. Moreover, the velocity distribution did not show any increase of population at the expected velocity of the meteor shower. Therefore, for all practical purposes, we can ignore the existence of the Leonid shower on 19 November 2002 and take our results as those corresponding to the season. Similar results were also observed in November 2001 (not shown here) indicating that there is no annual variability, at least, between November 2001 and November 2002.

We have shown that the majority of echoes come from the Apex at different times during the same day and at different seasons. In order to save space and simplify our presentation, in Fig. 10 we show bivariate angular velocity distributions (East-West vs. North-South) with respect to the Apex location for the Leonid night and control night. Knowing where the Apex occurs at a given time, we have removed the Apex vector location from the vector radiant of meteors, i.e. we have plotted their velocity direction relative to the Apex in the same set of coordinates as in the sky maps (NS and EW angles).

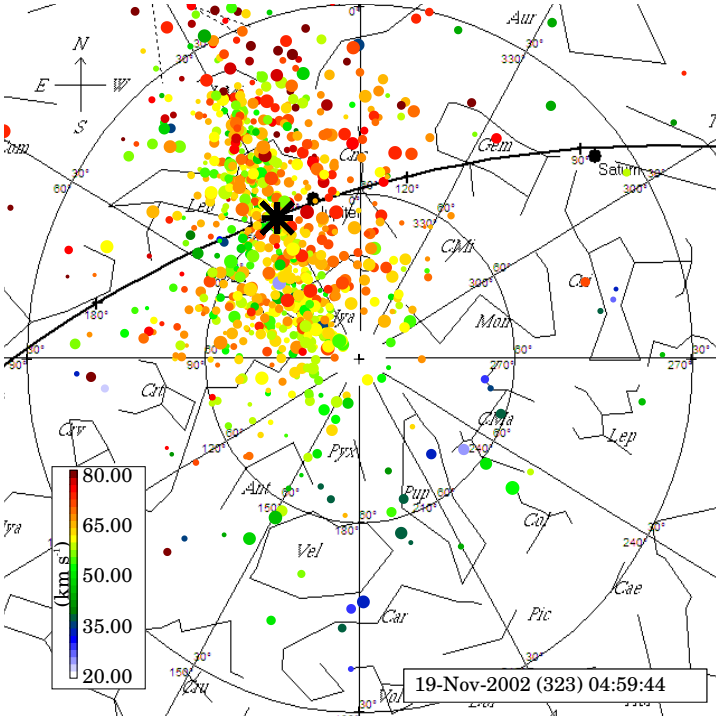

Fig. 7. Skymap distribution of meteor radiants around 05:00 LT during the Leonid night of 19 November 2002. The absolute velocity is color-coded while the SNR is represented by the size of the circles. The Ecliptic plane projected into the celestial sphere is shown with a black curve, and the Earth's Apex with thick asterisk.

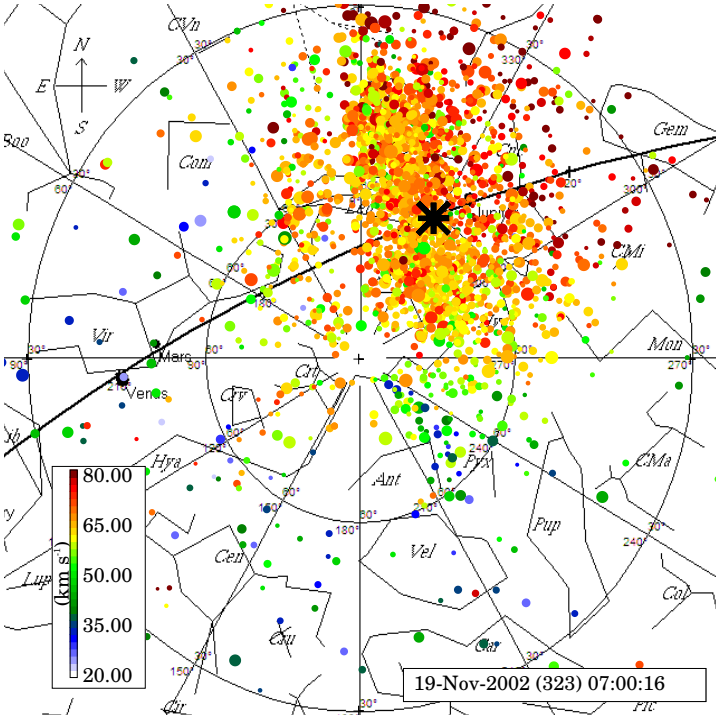

Fig. 8. Skymap distribution of meteors similar to Fig. 7 but around 07:00 LT.

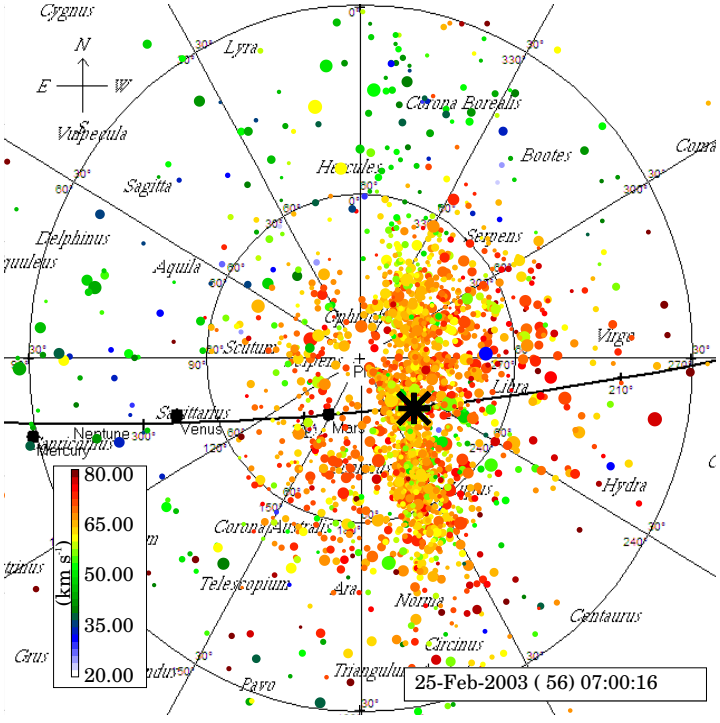

Fig. 9. Skymap distribution of meteors similar to Fig. 7 but for a control night around 07:00 LT on 25 February 2003.

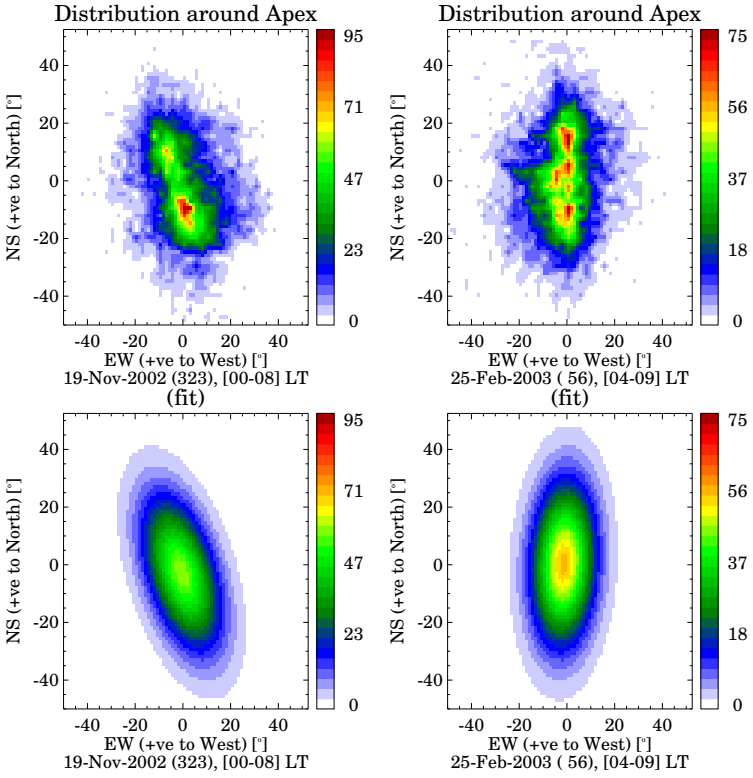

Fig. 10. Angular velocity distribution of meteors around the Apex for the Leonid night (left) and control night (right). Bottom panels show the fitted distributions using two-dimensional Gaussian functions.

In addition, we have fitted a two-dimensional Gaussian function to the bivariate distributions (bottom panels). Note that the distributions are oriented as expected from Figs. 7, 8 and 9. The orientation depends on the position of the Ecliptic plane.

The main parameters of these distributions are presented in Table 2. The rotation angle of the fitted distributions represents the rotation of the minor axis with respect to the EW axis (positive counter clockwise). There is very good agreement between the widths of the Leonid night and control night distributions. Furthermore, the rotation angles agree with the axis of the Ecliptic plane. Our results can be taken as the distribution of the meteors for the epochs selected (similar results have been obtained also in June and August 2003, not shown here). The Leonid population appear to affect only the large meteors which are visible optically and which seldom cross our 1° beam.

Therefore our results indicates that the velocity distribution of meteors with respect to the Earth's frame of reference is clustered around the Earth's Apex, within ±18° transverse to the Ecliptic and narrow (±8.5°) in heliocentric longitude in the Ecliptic plane, independent of season.

By removing the Earth velocity around the Sun ($\sim$29.8 km s^{-1}) the mean widths of the velocity distributions almost doubles (e.g. from 8.88° to 15.23° and from 18.05° to 32.00° for the November event) and remain clustered around the Apex moving on a retrograde direction.

Although Jicamarca is one of the few radars able to determine the three-dimensional velocity vector, we think our results can be extrapolated to other latitudes and possibly to radars working at other frequencies. For example, the recent observations done with the Arecibo radar using two beams (Janches et al., 2003) are in excellent agreement with our results and the interpretation has to be worked out accordingly. Moreover, even when much narrower beams are used, one has to be aware that the majority of meteors are probably coming from the Apex, as in our case, and therefore not necessarily coming along the beam as assumed by Mathews et al. (1997). Knowing the source, we have been able to correct significantly our radial acceleration which in turn has implication on the controversial radar measurements of meteor mass flux (Mathews et al., 2001).

5 Summary and conclusions

As it has been shown in previous sections, we have successfully implemented a technique to observe and characterize meteor head echoes at equatorial latitudes. The use of the large power-aperture capabilities at Jicamarca has allowed us to observe a high rate of meteors (more than 3000 per hour) in the small volume subtended by the 1° antenna-beam. Moreover, using interferometry, we have been able to characterize the three-dimensional components of meteor velocities in the Earth's frame of reference.

Our results do not show any evidence of the Leonid meteor showers, in agreement to results reported by other large power-aperture radars (e.g. Janches et al., 2000; Pellinen-Wannberg et al., 1998; Sato et al., 2000). We have shown that meteor parameters during both Leonid and control nights are statistically similar (range of occurrence, velocity distribution, deceleration distribution, origin). Apparently, we detect only the very small sporadic meteors, which are much more abundant than the larger meteors associated with major meteor showers optically observed and which seldom cross the 1° antenna beam.

Besides providing meteor-head observations at a unique frequency (50 MHz) and location (equatorial latitudes), our results are particularly important for the 3-D characterization of meteor heads. We have shown, at different seasons with negligible annual variation, that the velocity distribution of meteors with respect to the Earth's frame of reference is clustered around the Earth's Apex, within ±18° transverse to the Ecliptic and narrow (±8.5°) in heliocentric longitude in the Ecliptic plane. A change to a solar inertial frame of reference, roughly double the widths of these distributions, since most of the meteors have a relative velocity in a retrograde direction which is about twice the orbital velocity of the Earth. The velocity representation in heliocentric coordinates including the gravitational attraction as well as its orbital distribution will be left for a future effort.

So far, our observations have been concentrated around sunrise times when the EEJ echoes are expected to be absent or weak. In the future, we plan to extend our observations to other times, particularly during daytime counter electrojet conditions when EEJ are also expected to be weak. Moreover, we plan to continue improving the technique in order to get better time coverage as well as more precise parameters.

Acknowledgements. We thank D. Janches, M. Oppenheim, T. Sato, M. Sulzer, and Q. Zhou for their fruitful comments and suggestions in early stages of this work. We thank the Jicamarca staff for performing the observations, particularly M. Milla for helping with the processing and analysis. The Jicamarca Radio Observatory is operated by the Instituto Geofísico del Perú, with support from the NSF Cooperative Agreement ATM-9911209 through Cornell University.

Edited by: D. Janches

References

Chapin, E. and Kudeki, E.: Radar interferometric imaging studies of long-duration meteor echoes observed at Jicamarca, J. Geophys. Res., 99, 8937–8949, 1994.

Close, S., Hunt, S. M., McKeen, F. M., and Minardi, M. J.: Characterization of Leonid meteor head echo data collected using the VHF-UHF advanced reserach projects agency long-range tracking and instrumentation radar (ALTAIR), Radio Sci., 37, doi:10.1029/2000RS002602, 2002a.

Close, S., Oppeheim, M., Hunt, S., and Dyrud, L.: Scattering characteristics of hig-resolution meteor head echoes detected at multiple frequencies, J. Geophys. Res., 107, doi:10.1029/2002JA009253, 2002b.

Dyrud, L. P., Oppeneheim, M., Close, S., and Hunt, S.: Interpretation of non-specular radar meteor trails, Geophys. Res. Lett., 29, doi:10.1029/2002GL015953, 2002.

Farley, D. T.: On-line data processing techniques for MST radars, Radio Sci., 20, 1177–1184, 1985a.

Farley, D. T.: Theory of equatorial electrojet plasma waves: New developments and current status, J. Atmos. Sol. Terr. Phys., 47, 729–744, 1985b.

Hocking, W. K., Fuller, B., and Vandepeer, B.: Real-time determination of meteor-related parameters utilizing modern digital technology, J. Atmos. Sol. Terr. Phys., 63, 155–169, 2001.

Hunt, S. M., Oppenheim, M., Close, S., Brown, P. G., McKeen, F., and Minardi, M.: Determination of the meteoroid velocity distribution at the Earth using high-gain radar, Icarus, 168, 157–169, 2004.

Janches, D., Mathews, J. D., Meisel, D. D., and Zhou, Q. H.: Micrometeor observations using the Arecibo 430 MHz radar i. determination of ballistic paramater from measured Doppler velocity and deceleration results, Icarus, 145, 53–63, 2000.

Janches, D., Nolan, M. C., Meisel, D. D., Mathews, J. D., Zhou, Q. H., and Moser, D. E.: On the geocentric micrometeor velocity distribution, J. Geophys. Res., 108, doi:10.1029/2002JA009789, 2003.

Mathews, J. D., Meisel, D. D., Kunter, K. P., Getman, V. S., and Zhou, Q. H.: Very high resolution studies of micrometeors using the Arecibo 430 MHz radar, Icarus, 126, 157–169, 1997.

Mathews, J. D., Janches, D., Meisel, D. D., and Zhou, Q. H.: The micro-meteoroid mass flux into the upper atmosphere: Arecibo results and a comparison with prior estimates, Geophys. Res. Lett., 28, 1929–1932, 2001.

Pellinen-Wannberg, A., Westman, A., Wannberg, G., and Kaila, K.: Meteor fluxes and visual magnitudes from EISCAT radar event rates: A comparison with cross-section based magnitudes estimates and optical data, Ann. Geophysicae, 116, 1475–1485, 1998.

Rihaczek, A. W. and Golden, G. M.: Range sidelobe suppression fro barker codes, IEEE Trans. Aerosp. Electron Sys., AES-7, 1087–1092, 1971.

Sato, T., Nakamura, T., and Nishimura, K.: Orbit determination of meteors using the MU radar, IEICE Trans. Commun., E83-B, 1990–1995, 2000.

Wannberg, G., Pellinen-Wannberg, A., and Westman, A.: An ambiguity-fuction-based method for anlaysis of doppler decompressed radar signals applied to EISCAT measurements of oblique UHF-VHF meteor echoes, Radio Sci., 31, 497–518, 1996.

Woodman, R. F.: Inclination of the geomagnetic field measured by an incoherent scatter technique, J. Geophys. Res., 76, 178–184, 1971.

Woodman, R. F.: Spectral moment estimation in MST radars, Radio Sci., 20, 1185–1195, 1985.

Zhou, Q. H., Perillat, P., Cho, J. Y. N., and Mathews, J. D.: Simultaneous meteor echo observations by large aperture VHF and UHF radars, Radio Sci., 33, 1641–1654, 1998.